JOURNAL OF AIRCRAFT
Vol. 46, No. 1, January–February 2009

Residual-Strength Assessment of Modified Transport Aircraft Fuselages

Y. Yamada* and T. Lacy Jr.†
Mississippi State University, Starkville, Mississippi 39762
and
J. Luzar‡
Spirit AeroSystems, Wichita, Kansas 67210

DOI: 10.2514/1.35678

In this study, several combinations of fail-safe features were investigated to assess their effect on the damage-tolerance characteristics and residual strength of a typical military transport aircraft fuselage section composed of floating-frame construction. Detailed nonlinear finite element models were developed for a key area of a representative aft fuselage. These local fuselage models were refined to include longitudinal lead and multiple-site-damage cracks of various sizes. A global-to-local modeling procedure was used whereby kinematic boundary conditions applied to the edges of the local fuselage models were developed using internal field quantities from a finite element simulation of a structurally complete (global) fuselage for a given load case. A residual-strength assessment of the relevant aft section for load cases involving a combination of limit internal pressure and flight loads was conducted using highly refined finite element models for cases involving 1) no fail-safe features (i.e., the basic fuselage configuration), 2) inclusion of shear ties as part of a modified fuselage design, 3) inclusion of tear straps as part a modified fuselage design, and 4) inclusion of both shear ties and tear straps. The influence of discrete source damage and small-scale cracking at fastener holes (i.e., multiple-site damage) was considered in the analysis. The critical crack-tip opening-angle fracture criterion and plane-strain core concept were employed in performing large-deformation elastic–plastic stable-tearing analyses using three-dimensional fracture-analysis code and structural analysis of general shells code to predict the fuselage section's residual strength. These results suggest that shear ties and tear straps may be effectively used to increase the structural integrity of the aft fuselage. Key results from this study may provide useful information regarding the efficiency of incorporating fail-safe design modifications in the existing aircraft to enhance the residual strength of cracked sections of the fuselage.

I. Introduction

BECAUSE of the high cost of new commercial and transport air vehicles, many operators attempt to maintain their existing fleet of aircraft for as long as possible. As metallic airplanes age, certain measures must be taken to ensure structural integrity. Arguably, airframe structural integrity may be determined from an assessment of the residual strength, rigidity, damage tolerance, and durability characteristics [1,2]. *Residual strength* may be defined as the amount of static strength available at any time during a specified service period considering that damage exists in the structure and will grow as a function of in-service loading. *Damage tolerance* may be defined as the ability of a structure to sustain damage associated with cracks, fatigue, and corrosion. An improvement in fuselage damage-tolerance properties may be attained by incorporating fail-safety features (i.e., redundant load paths) in combination with crack arresters (e.g., tear straps and shear ties); such design modifications may enhance the service life of a given aircraft. Through proper implementation of a damage-tolerance plan involving periodic inspections, any subcritical fatigue cracks, discrete source damage, and/or corrosion will likely be detected and repaired before the expiration of the intended service life.

Primary structural assemblies may be modified to include fail-safe design features that allow the structure to sustain levels of discrete source damage, fatigue cracks, and/or corrosion that were not accounted for in the original design process [3,4]. Fuselage structures are especially susceptible to the formation of longitudinal skin cracks induced by cyclic internal pressure loads and/or normal flight loads. Aging aircraft may develop fatigue cracking and/or corrosion near riveted areas in overlapping skin panels.

In the latter stages of the intended service period (or if the design service life is extended), the onset of widespread fatigue damage (WFD) near mechanically fastened areas may significantly reduce the residual-strength and/or damage-tolerance properties of metallic fuselage structures [5]. WFD may be defined by the simultaneous presence of cracks in multiple layered sections in a fuselage structure. Depending on the size and density of WFD cracks in an aging aircraft, primary structural components may not retain the requisite residual strength necessary to avoid a catastrophic failure [6]. Incorporation of crack arresters (e.g., shear ties and tear straps) may be one of the most effective ways to stall or reduce lead-crack propagation rates due to the presence of WFD (i.e., improve damage tolerance).

The original design of certain older tanker/transport aircraft fuselages (Boeing 707, KC-135, etc.) was primarily composed of aluminum-skin panels, longitudinal stringers, and floating frames. Although typical fail-safe features were not included as part of the initial design of these aircraft, the original (basic) fuselage design was determined to be sufficient to meet military damage-tolerance requirements over the course of the *original* aircraft service lives [7–9]. Also, periodic inspections of principal structural elements were required to ensure flight safety.

Although an assessment by the U.S. Air Force (USAF) suggested that these aircraft could remain in service beyond their *original* design life, the possibility of fatigue-damage development and/or corrosion was not considered in the initial USAF evaluation.

Received 14 November 2007; revision received 14 February 2008; accepted for publication 29 February 2008. Copyright © 2008 by the American Institute of Aeronautics and Astronautics, Inc. All rights reserved. Copies of this paper may be made for personal or internal use, on condition that the copier pay the $10.00 per-copy fee to the Copyright Clearance Center, Inc., 222 Rosewood Drive, Danvers, MA 01923; include the code 0021-8669/09 $10.00 in correspondence with the CCC.

*Graduate Student, Department of Aerospace Engineering. Student Member AIAA.
†Associate Professor, Department of Aerospace Engineering, Mail Stop 9549. Associate Fellow AIAA.
‡Senior Damage Tolerance Engineer.

Because older tanker/transport aircraft were designed and built before the establishment of modern damage-tolerance and fail-safety concepts, a review of initial structural integrity evaluations and early fail-safe tests involving similar aircraft was conducted by Cope [10] to identify possible critical fuselage areas. Based on this review, a highly refined local finite element model [10] was developed for a representative fuselage for which the geometry represented a subset of a larger global model (cf. Fig. 1). Arguably, such local models will adequately characterize the fracture behavior of cracked fuselages, provided that the models are sufficiently large to avoid any interaction between the crack and the model boundaries [11].

The boundary conditions applied in the local models were interpolated from internal-surface field quantities from a global model containing no cracks. Cope [10] performed material and geometric nonlinear analyses of each fuselage section aimed at residual-strength determination as a function of crack configuration for key areas of a typical forward, center, and aft fuselage (cf. Fig. 2). It was concluded that the aft-fuselage section posed the greatest risk because of the relatively low fracture toughness and thickness of the skin material employed in that region (cf. Fig. 2). It was recommended that modifications to the basic fuselage design (i.e., inclusion of shear ties, tear straps, and/or fail-safe chords) should be considered to enhance an aircraft's damage-tolerance characteristics. Such fail-safe features are commonly employed in modern transport fuselage designs.

Similar to the KC-135 and 707, the idealized aircraft considered in this study has semimonocoque D-shaped fuselage construction, where only the upper half of the cylindrical fuselage is pressured (cf. Fig. 1). A nominal 72-in.-radius fuselage was assumed with longitudinal stringers mechanically fastened to an aluminum skin. Each fuselage is reinforced by a series of periodically spaced floating frames (typical frame spacing of 20.0 in.). In standard floating-frame construction, the frames are attached to the skin only at the stringer/frame fastener interconnections. Because typical stringer spacings are on the order of 8–9 in., the frames are relatively ineffective as crack arresters or crack stoppers for longitudinal skin cracks. Figure 3 shows a schematic of the representative fuselage as well as a typical skin/stringer/floating-frame interconnection. Standard body-station (BS), butt-line (BL), and water-line (WL) systems for identifying the x, y, and z coordinates of points within the aircraft (cf. Fig. 3) are employed. Stringers are numbered sequentially on the left- and right-hand sides of the aircraft, beginning at the crown of the aircraft, denoted by S-01 (BL 0.0), S-02R, S-03R, etc., as indicated in Fig. 3.

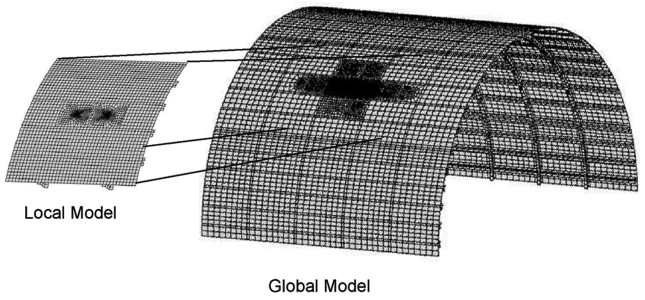

Fig. 1 Local and global models [10,11].

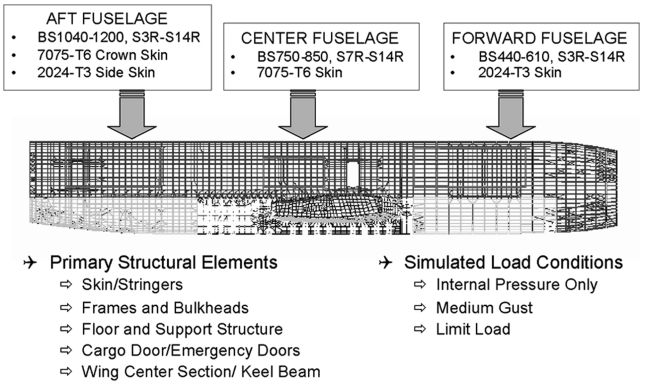

Fig. 2 Three key areas of the representative fuselage considered by Cope [10].

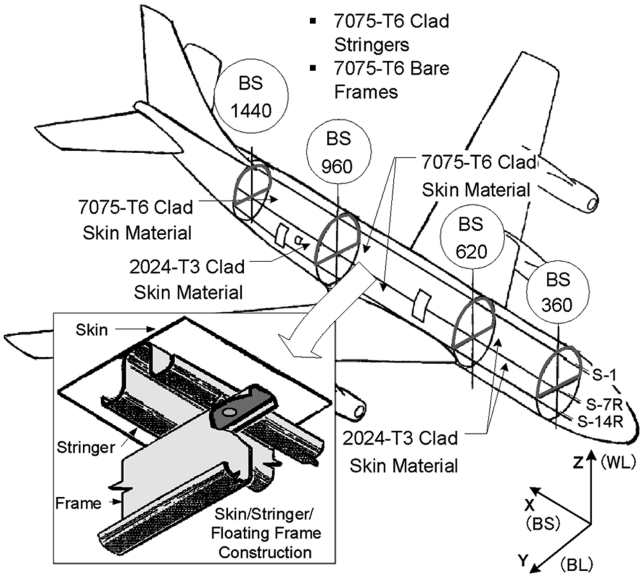

Fig. 3 Fuselage construction of representative tanker/transport.

In contrast to other common tanker aircraft, the fuselage considered in this study incorporates no fail-safe features such as tear straps and/or shear ties. In addition, this aircraft has a noncylindrical D-shaped pressurized fuselage. Although modern transport fuselage designs generally incorporate skins composed entirely of 2024-T3 aluminum, the center and aft-fuselage sections of certain older tanker/transport aircraft consist of 7075-T6-clad skin panels. It is commonly accepted that 2024-T3 is the preferred skin material because it has a higher fracture toughness value than 7075-T6.

A linearly elastic finite element model of the entire idealized fuselage was developed to determine internal structural loads for critical fuselage areas for a wide variety of load cases [9]. This model contained representations of all of the primary structural components such as skin, stringers, frames, bulkheads, floor sections, wing center section, and wing-to-body connection. In addition, estimated field quantities evaluated along internal surfaces in the air vehicle model were used to establish boundary conditions for detailed local models simulating cracked sections of the fuselage [10] for load cases involving internal pressure and/or flight loads. The flight loads are equivalent to two-thirds of an ultimate dive maneuver load condition for a 275,000 lb gross weight aircraft [7]. Limit-load pressure loading, which represents the maximum operating pressure that the fuselage structure is likely to see in its service life [7], was considered.

In this research, several combinations of fail-safe features were investigated to assess their effect on the damage-tolerance characteristics and residual strength of the tanker/transport *aft* fuselage section for load cases involving both internal pressure and critical flight loads. A residual-strength assessment of the relevant aft section of the representative fuselage was conducted using highly refined finite element models. The influence of discrete source damage and small-scale cracking at fastener holes [i.e., multiple site damage (MSD)] was considered in the analysis. The critical crack-tip opening angle (CTOA) fracture criterion [12] was employed in performing elastic–plastic stable-tearing analyses to predict the fuselage section's residual strength. Key results from this study may provide useful information regarding the efficiency of incorporating fail-safe design modifications in aircraft with floating-frame construction to enhance the residual strength of cracked sections of the fuselage.

II. Analysis Method

Fracture mechanics analyses of metallic aircraft structures often involve the use of linear elastic fracture mechanics (LEFM) handbook solutions for stress-intensity factors (SIFs) for idealized structural geometries, such as that for a single crack emanating from a fastener hole in a flat plate. However, fracture analyses of transport fuselage structures with semimonocoque construction arguably should account for large displacements, elastic–plastic material behavior, and the possible existence of MSD cracks to accurately assess structural integrity [13]. In this work, two fracture mechanics codes, three-dimensional fracture-analysis code (FRANC3-D) [14] and structural analysis of general shells (STAGS) code [15], were used to simulate the nonlinear fracture behavior of cracked sections of the representative military transport fuselages.

FRANC3-D [14] was developed for simulating discrete crack propagation in stiffened curvilinear thin-shell structures under either elastic or elastic–plastic conditions. Essentially, FRANC3-D is a pre- and postprocessor for the nonlinear shell code STAGS [15]. FRANC3-D may be used to establish finite element representations of thin-walled semimonocoque structures, define crack configurations, and perform adaptive remeshing and/or nodal release techniques necessary to simulate evolving cracks. FRANC3-D is well suited to trace structural geometry evolution due to propagation of single or multiple cracks [16–19]. STAGS is a finite element solver developed by Lockheed Martin Aerospace Corporation and NASA [15] to analyze large-deformation inelastic shell buckling.

STAGS may be used to conduct strength, stability, and collapse analyses of general shell structures with complex geometry subjected to combined loadings. STAGS can be used to calculate linear and nonlinear elastic strain energy release rates for multiple interacting cracks that can be used to determine mixed-mode phenomena at the crack tips in FRANC3-D, which can then be used in a damage-tolerance evaluation of a fuselage structure. FRANC3-D has been integrated with STAGS to estimate crack-tip fracture parameters and/or residual strength based upon either LEFM or elastic–plastic fracture mechanics (EPFM) concepts.

As the fracture process progresses, intense inelastic deformation in the vicinity of a crack tip may result in crack-tip stresses that are drastically lower than those predicted by LEFM; the presence of material inelasticity and/or plasticity will generally increase the material's resistance to crack extension. As the size of the crack-tip plastic zone becomes large in comparison with the K_I-dominated (or J_I-dominated) zone, however, the crack-tip stresses based upon LEFM cease to be valid and the SIF no longer represents a viable fracture parameter (i.e., application of LEFM is questionable). Newman [20] demonstrated, however, that the critical value of CTOA may be reliably used to predict the onset of stable-tearing behavior and residual strength for materials with relatively large degrees of crack-tip plasticity. When implementing the CTOA concept, it is assumed that crack extension will occur whenever the opening angle formed by the upper and lower crack faces reaches some critical value [21]. The CTOA [or, equivalently, the crack-tip opening displacement (CTOD)] is commonly defined at some fixed distance d behind the crack tip (cf. Fig. 4). The CTOA for the mode I case is defined as

$$\text{CTOA} = 2 \cdot \tan^{-1} \frac{\delta}{2d} \tag{1}$$

where δ is the CTOD measured at a specific distance d behind the moving crack tip. A fixed value of $d = 0.04$ in. is commonly used throughout the literature [22]. In this research, however, the length

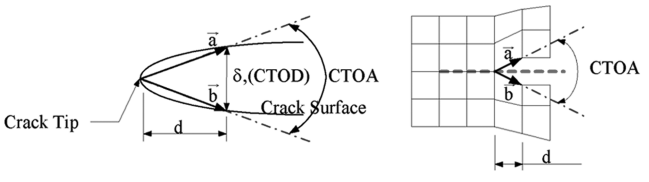

Fig. 4 CTOA definition.

$d = 0.05$ in. was used in the numerical evaluation of the CTOA as well as to define the finite element edge lengths along the crack growth path to ensure consistency with Cope [10].

The opening angle for the mixed-mode case may be obtained from the cross product of two vectors:

$$\text{CTOA} = \sin^{-1} \frac{\|\mathbf{a} \times \mathbf{b}\|}{\|\mathbf{a}\| \cdot \|\mathbf{b}\|} \tag{2}$$

where **a** and **b** are vectors for which the origin corresponds to the crack tip and for which the tips correspond to points located at a distance d along the deformed upper and lower crack faces, respectively. For pure mode II (sliding) deformation, the crack-face sliding displacement is used to establish an equivalent CTOA for use in assessing crack extension. Calculated values of CTOA at a crack tip of interest for a given prescribed load level are compared with the critical values necessary to extend the crack. For the 2024-T3 and 7075-T6 aluminum skins considered in this research, a piecewise linear stress–strain curve was used to approximate the elastic–plastic material behavior (cf. Fig. 5).

There are several key issues that must be addressed when numerically implementing the CTOA concept to predict the fracture behavior of thin-walled metallic structures. Although use of two-dimensional (2-D) elements facilitates the development of tractable finite element models, the fracture process is intrinsically a three-dimensional (3-D) process. Three-dimensional constraint effects in the vicinity of the crack tip drastically influence the crack-face opening behavior as well as crack extension; the CTOA is generally not constant through the thickness. Use of 2-D plane-stress elements arguably cannot adequately simulate the physics of a fracture process that may involve severe crack tunneling in thin-sheet materials. Dawicke et al. [23] used 3-D finite element analysis of crack extension in relatively thick and thin metals to demonstrate that the effect of the crack-tip constraint must be accounted for to obtain accurate failure predictions using constant critical CTOA values. Newman [20] and Dawicke et al. [23] showed that the constraint around the crack tip due to metal plasticity may be simulated using 2-D plate or shell elements by employing the plane-strain core concept.

In such an approach, 3-D constraint conditions around a crack tip may be simulated in 2-D analyses by employing plane-strain elements within some distance h_c of the crack plane. The plane-strain core models the high constraint around a crack tip but allows for the widespread plastic, yielding under plane-stress conditions away from the crack tip. In this study, plane-stress conditions were assumed everywhere in the model except for two rows of elements on both sides of predefined crack location, as illustrated in Fig. 6. The height of the plane-strain core, h_c, was selected to be equal to or less than the thickness of the plate. Also, a fixed distance d behind a crack tip for CTOA should be consistent to the plane-strain core height. Using the plain-strain core concept, an elastic–plastic stable-tearing analysis was performed. A nodal release method and a load relaxation technique were used to extend a crack while the shell is in a

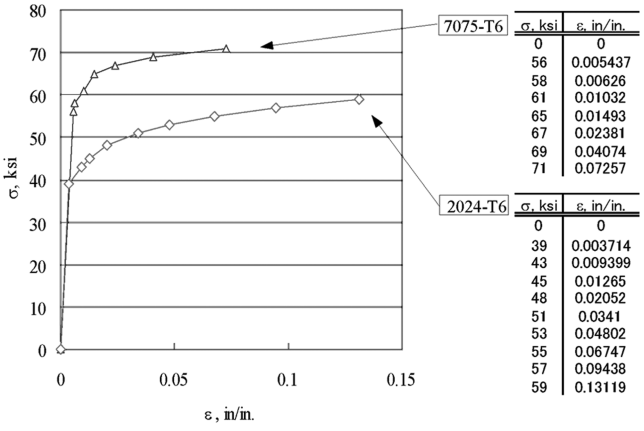

Fig. 5 Piecewise linear stress–strain curves for 7075-T6 and 2024-T3 aluminum alloys.

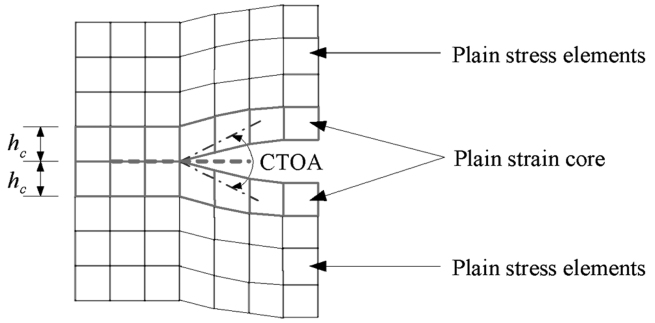

Fig. 6 Plain-strain core concept.

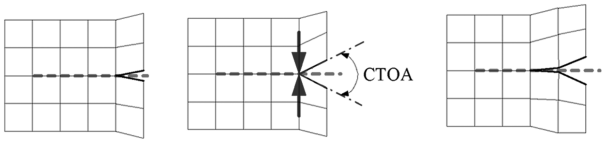

a) Predefined crack path **b) Satisfy CTOA, and replaced with force to hold nodes closed** **c) Newly introduced longer crack**

Fig. 7 Mechanism of nodal release method in STAGS.

nonlinear equilibrium state based upon the modified crack-closure method [24].

Once the calculated CTOA at a crack tip reaches the critical value, the nodal displacement compatibility condition at the given crack tip is replaced with equivalent crack-tip forces required to hold the current crack-tip nodes together, as shown in Fig. 7. The equivalent crack-tip forces are gradually reduced to zero to establish a new equilibrium state corresponding to the longer crack configuration. This process may be continued until the lead-crack tip reaches the next fastener geometric locations or links up with a MSD-crack tip, because crack linkup may cause an unstable crack extension. In the case with no MSD, analyses were stopped whenever the crack tip reached a rivet location. The residual strength of the structure can be determined from the far-field load condition at which the linkup occurred in the stable-tearing analysis.

Modeling of mechanical fasteners is an important factor in obtaining accurate estimates of the stress field in a mechanically fastened joint containing a lead crack and MSD. Consistent with the methodology proposed by Young et al. [24], Chen et al. [5], and Carter et al. [14] and implemented by Cope [10], two-noded spring elements were used to simulate the fastener load transfer between mating aluminum sheets in a cracked lap joint. The fastener holes were not modeled. Three rows of two-noded six-degree-of-freedom spring-rivet elements were used to model the 0.1875-in.-diam. aluminum rivets at the lap joint. The rivet properties were computed

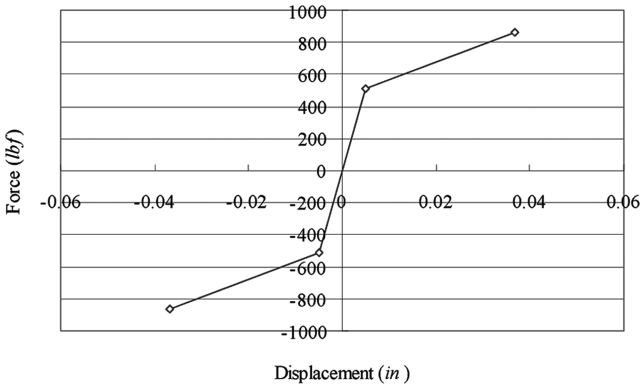

Fig. 8 Nonlinear fastener shear force-displacement relationship.

using a spring element fastener representation developed by Cope and Lacy [25].

Consistent with [18,24,26], it is assumed that the nonlinear transverse shear force-displacement response could be approximated using a piecewise linear approximation based on experimental data; the fastener response associated with axial extension, torsion, and bending was assumed to be linearly elastic. Figure 8 shows the idealized fastener transverse shear force-displacement relationship for a typical 0.1875-in.-diam. aluminum rivet. The initial elastic stiffness and subsequent tangent (plastic) stiffness are 105.2 and 23.4 klb/in., respectively. The axial, torsion, and bending stiffnesses are 140.0 klb/in., 231.1 in.$^2 \cdot$ lbf/rad, and 557.7 klb/in., respectively.

III. Damage Tolerance and Residual Strength of Fuselage Fail-Safe Design Model

One primary objective of this research was to investigate the effect of fail-safe design modifications (i.e., inclusion of tear straps, shear ties, and/or fail-safe chords) on the structural integrity of the aft floating-frame fuselage structure. The basic fuselage construction consisted of 2024-T3-clad aluminum-skin panels mechanically fastened to 7075-T6 longitudinal stringers; the skin/stringer assemblies were mechanically fastened to circumferentially oriented 7075-T6 bare floating frames at the stringer/frame interconnections, as illustrated in Fig. 9. As a consequence of the floating-frame construction, the basic structure provided relatively limited resistance to longitudinal crack propagation.

The second idealized fuselage structural configuration was reinforced with 0.05 in. 7075-T6-clad shear-tie angles mechanically fastened directly to the skin at frame sections between stringers. The outer flanges of the standard Z-shaped frames were reinforced with a combination of circumferentially oriented structural angles (fail-safe chords) and reinforcing straps composed of 0.05-in.-thick bare 7075-T6, as illustrated in Fig. 10. The shear ties arguably act as crack

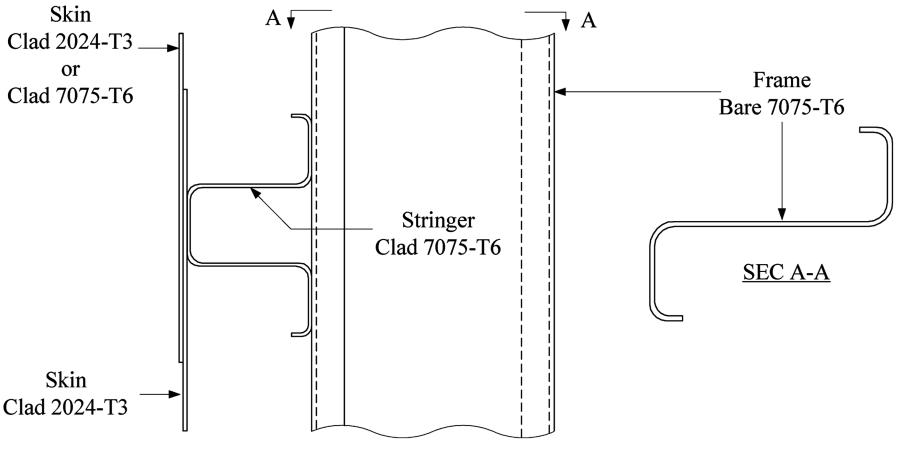

Fig. 9 Cross section for the floating-frame fuselage basic model.

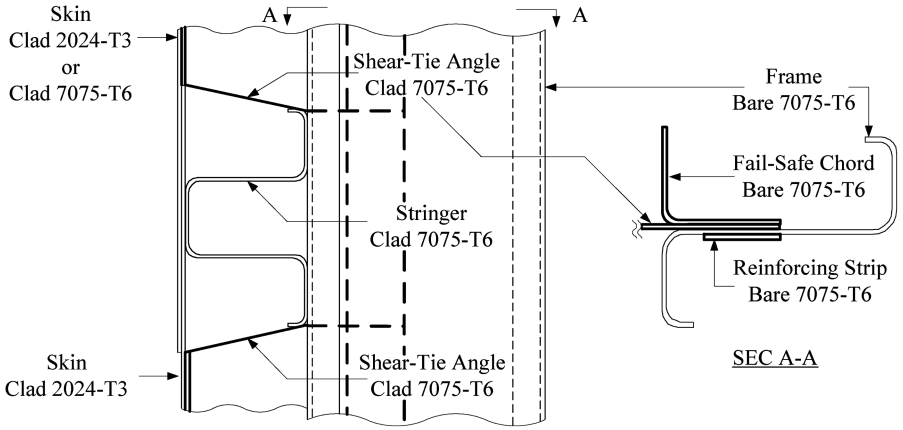

Fig. 10 Cross section for the fuselage shear-tie model.

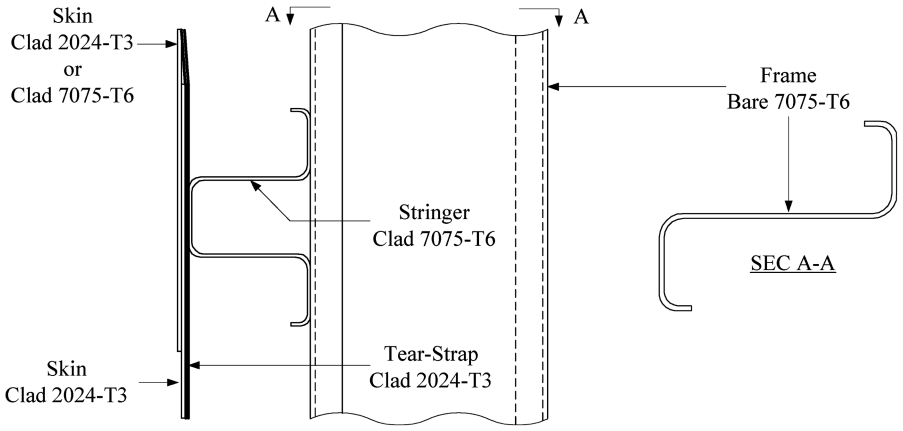

Fig. 11 Cross section for the fuselage tear-strap model.

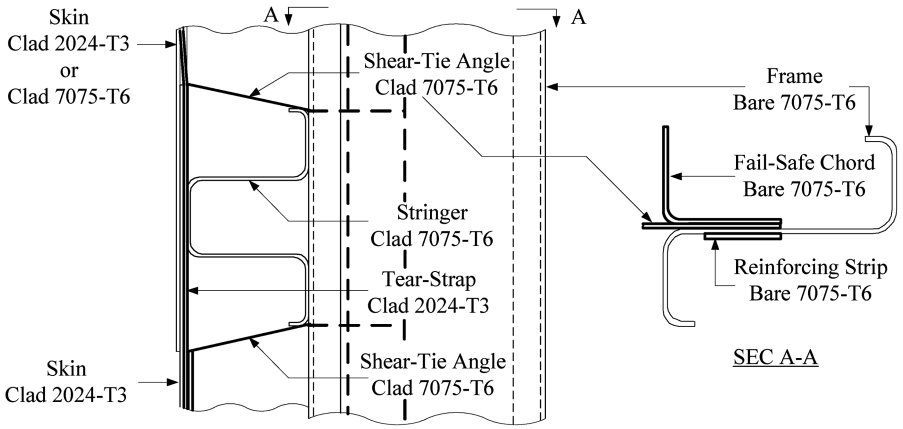

Fig. 12 Cross section for the fuselage combination model.

stoppers because they provide a means for stress redistribution from the cracked skin to the frames; in addition, they may serve to inhibit the mode I opening displacement of skin cracks. The skin of the third idealized fuselage structural configuration was reinforced with mechanically fastened, circumferentially oriented, 4-in.-wide tear straps composed of 0.032-in.-thick clad 2024-T3. The centerline-to-centerline spacing of the tear straps was 10 in; tear straps were positioned along the frame centerlines and centerline of the midsection between frames, as illustrated in Fig. 11.

Because the tear straps directly reinforced the skins, they also provided significant longitudinal crack stopping capability. Note that because the tear straps were located at the frame locations and at the frame midbays, the longitudinal spacing between the tear straps (10 in.) was one-half that associated with the shear ties (20 in.). Hence, the use of tear straps may provide somewhat better resistance to crack extension than the use of shear ties. In addition, a fourth structural configuration was simulated that involved incorporation of *both* shear ties and tear straps. The combination model accounted for the reinforcement due to shear ties, fail-safe chords, reinforcing straps, and tear straps (cf. Fig. 12). In the latter model, the shear ties were attached directly to the tear straps, rather than to the skin. The purpose of these models was to verify which structural modification had the greatest beneficial impact on the fuselage damage-tolerance characteristics.

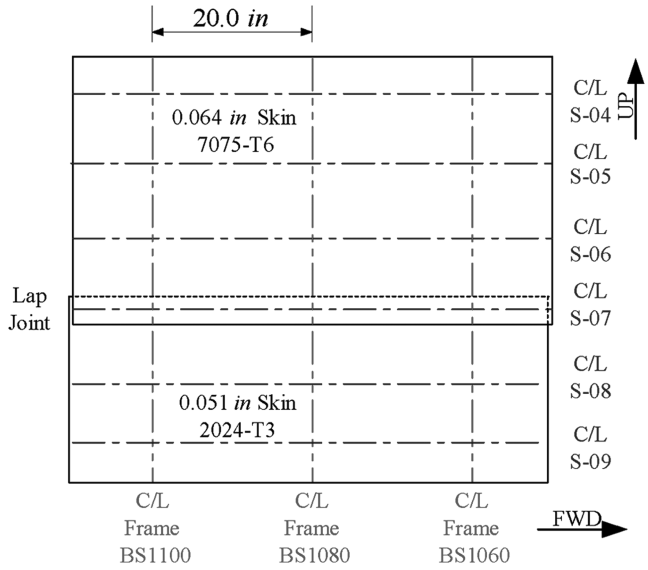

Fig. 13 Aft-fuselage panel configuration for fail-safe-features analysis.

To assess the beneficial effect associated with incorporation of fail-safe design features (i.e., tear straps and shear-tie angles) in the aft section of the representative fuselage considered by Lacy et al. [26], a set of material and geometric nonlinear (elastic–plastic) stable-tearing analyses was performed to assess the residual strengths of the basic and reinforced aft-fuselage structures containing lead cracks of variable length as well as MSD cracks. The relative improvement in residual strength associated with incorporation of tear straps and/or shear-tie angles for cracked fuselages containing lead cracks and MSD can be used to determine the merits of each proposed structural modification; this represents the primary contribution of this work. In both sets of analyses, damage scenarios involving various combinations of lead-crack lengths and MSD-crack lengths subjected to limit-load fuselage pressurization and flight loads were investigated.

In these analyses, local aft-fuselage models were developed consisting of a longitudinal section of skin spanning between stringers S-04R, and S-09R (cf. Fig. 13). The aft-fuselage section contained a lap-joint section with three rows of mechanical fasteners (rivets) at S-07R joining the upper-crown 7075-T6-clad skin panel (thickness of 0.064 in.) and lower 2024-T3-clad skin panel (thickness of 0.051 in.). The lap-joint rivet diameter, longitudinal spacing, and circumferential spacing were 0.1875, 1.0, and 1.0 in., respectively. As a consequence, MSD cracks of length 0.05, 0.10, and 0.20 in. were considered in this work. Longitudinal lead cracks of varying initial crack length ($2a = 5.1$, 7.5, 9.9, 12.3, 14.7, 17.1, and 19.5 in.) and MSD cracks were centered about BS1080 in the upper fastener row at stringer S-07R.

A summary of the combinations of lead-crack lengths and MSD-crack lengths considered in this study is shown in Table 1. Note that in an elastic–plastic stable-tearing (residual strength) analysis, a significant plastic zone may form at the lead-crack and MSD-crack tips. For a dominant lead crack, a relatively large plastic zone may engulf several MSD sites 2–3 in. ahead of the lead-crack tip [27]. MSD cracks lying outside the plastic zone of the dominant lead crack have little effect on lead-crack extension/failure and can safely be neglected in the analysis [27–29]. Therefore, MSD cracks were only simulated at the first two fastener locations adjacent to the lead-crack tips.

Geometric nonlinear elastic finite element analyses of the local aft-fuselage basic structure with/without reinforcements were conducted using limit internal pressure load (11.47 psi) and prescribed kinematic boundary conditions (i.e., edge displacements and rotations) developed from a linearly elastic finite element model of a global fuselage [9]. These calculations showed that the mode I SIF was sufficiently large in comparison with the other calculated SIFs to warrant the assumption of self-similar crack extension in the forthcoming elastic–plastic fracture analyses for all of the structural configurations.

To evaluate the improvement in the fuselage residual strength due to the incorporation of fail-safe features (i.e., tear straps and/or shear ties), a total of 28 stable-tearing (elastic–plastic fracture) analyses were conducted for the four aft-fuselage structural configurations and lead-crack/MSD-crack combinations summarized in Table 1. Here, it was assumed that fast fracture was imminent after the lead crack coalesced with either an adjacent fastener hole or MSD crack. The far-field load (i.e., internal limit-load pressure with flight loads in this case) was expressed in terms of a nondimensionalized load factor. For example, a load factor of 1.0 suggests that 100% of the limit-load pressure with flight loads was required to initiate fast fracture (linkup) for a given crack configuration. Similarly, a load factor greater than 1.0 for a given crack configuration indicates that a *proportional* increase in the applied internal pressure and the flight loads is necessary for failure to occur. A load factor less than 1.0 suggests that unstable crack extension will occur at an applied load level *below* the requisite limit load.

For each lead-crack/MSD-crack combination, load factors were recorded every time a given lead crack linked up with an adjacent MSD crack or when a lead-crack tip advanced to the geometric location of the next adjacent fastener hole for cases with no MSD. Figure 14 contains a schematic of the combinations of lead cracks and MSD cracks considered in the analyses. Note that the center of each lead crack was offset by roughly one fastener location from the frame web at BS1080 (cf. Fig. 14); essentially, the cracks were centered about the circumferential row of fasteners defining the attachment between the shear-tie angles and the skin. In contrast, the tear straps were located symmetrically about the frame web, as shown in Fig. 14. As a consequence, the circumferential centerline of the center tear strap was offset by the fastener pitch from the center of the lead crack (i.e., the influence of the tear straps on the fracture behavior at each tip was slightly different). In the fuselage shear-tie and combination models, no shear-tie angles were simulated in the overlapping skin area of the lap joint. Circumferential tear straps in the idealized aft-fuselage tear-strap and combination models were simulated symmetrically about each frame web and at the midbay locations between frames (i.e., the tear straps were longitudinally centered every 10 in.). As suggested in Fig. 14, lead-crack lengths in excess of 17 in. resulted in at least one lead-crack tip residing *underneath* the adjacent midbay tear strap. Similarly, lead-crack lengths in excess of 12.3 in. resulted in at least one MSD crack located underneath the reinforcing midbay tear traps.

Residual-strength estimates, characterized in terms of the unit load factor, were determined for each structural configuration (basic, basic plus tear-strap reinforcements, basic plus shear-tie reinforce-

Table 1 Fuselage MSD damage scenarios for stable-tearing analysis

No. of fasteners with lead crack	Lead crack length $2a$, in.	MSD crack length, in.
5	5.1	0.00, 0.05, 0.10, 0.20
7	7.5	0.00, 0.05, 0.10, 0.20
9	9.9	0.00, 0.05, 0.10, 0.20
11	12.3	0.00, 0.05, 0.10, 0.20
13	14.7	0.00, 0.05, 0.10, 0.20
15	17.1	0.00, 0.05, 0.10, 0.20
17	19.5	0.00, 0.05, 0.10, 0.20

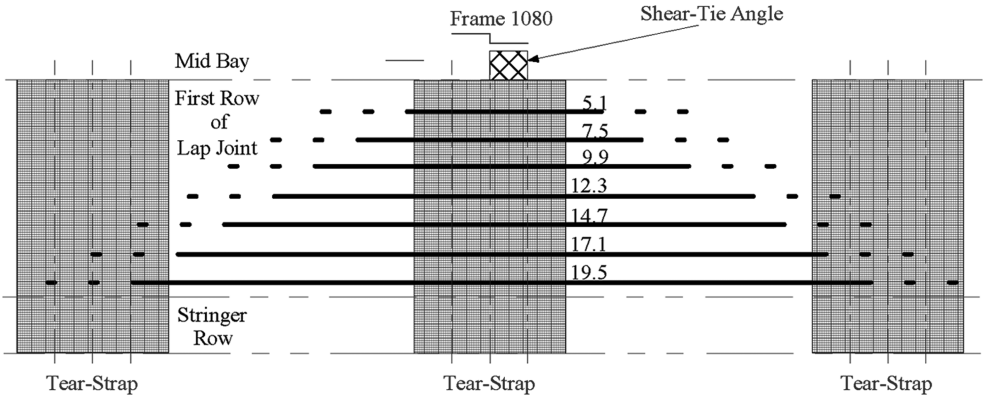

Fig. 14 Lap-joint crack locations for the fuselage combination model.

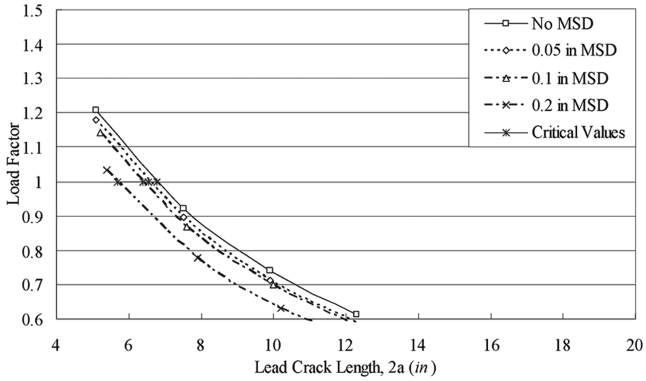

Fig. 15 Estimated residual strength of the representative basic aft fuselage.

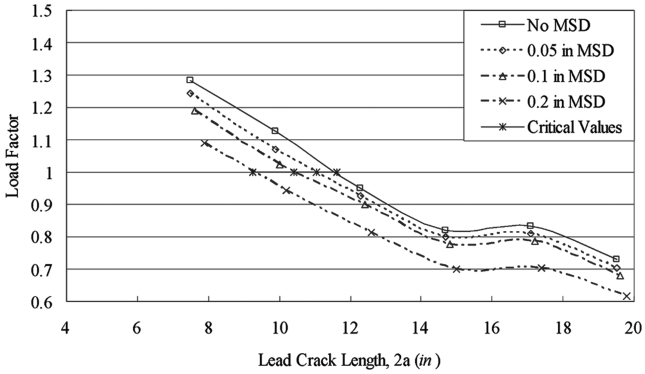

Fig. 16 Estimated residual strength of the representative aft fuselage with shear ties.

ments, and a combination of shear-tie and tear-strap reinforcements) as a function of lead-crack and MSD-crack lengths. Again, fast fracture was assumed to occur whenever the lead crack coalesced with an MSD crack or when the lead crack advanced to the nearest fastener-hole location. Figure 15 contains a plot of the residual strength as a function of lead-crack length and MSD-crack size for the unreinforced basic aft-fuselage configuration. Figures 16–18 contain similar residual-strength plots for the aft-fuselage section reinforced with shear ties, tear straps, and a combination of shear ties and tear straps, respectively.

Not surprisingly, the residual strength of the basic (unreinforced) aft-fuselage section containing a single lead crack decreased drastically with increasing lead-crack length, as shown in Fig. 15. The fuselage residual strength for lead cracks with lengths in excess of $2a \approx 6.8$ in. fell below a load factor of 1.0; this suggests that the cracked fuselage is unable to sustain the *required* loading without failure. The presence of MSD cracks only exacerbated the reduction in residual strength for a given lead-crack length. For example, the critical lead-crack lengths associated with MSD-crack lengths of 0.05, 0.10, and 0.20 in. were roughly $2a = 6.5$, 6.4, and 5.7 in., respectively. Hence, the critical lead-crack length for the case involving 0.20 in. MSD cracks was approximately 12.3% shorter than the non-MSD case. Alternatively, for a load factor of 1.0, the presence of 0.20 in. MSD cracks resulted in a 17.2% reduction in residual strength. This underscores the importance of accounting for the presence of MSD cracks when evaluating residual strength. Note that the combination of lead-crack lengths and MSD-crack lengths with a load factor of 1.0 defines the maximum level of damage that the aft fuselage can sustain while still carrying the required flight and pressurization loads. These values correspond to the intersection of the load-vs-lead-crack-length curves, with the horizontal line associated with a load factor of 1.0 (cf. Fig. 15).

Figure 16 shows a plot of the estimated residual strength as a function of lead-crack length for an idealized aft-fuselage section that has been reinforced with shear ties at the frame stations. Similar to the unreinforced (basic) aft-fuselage section, the estimated residual strength for a structure containing a single lead crack decreased with increasing lead-crack length, and the relative strength of the fuselage decreased with increasing MSD-crack sizes. The presence of the shear ties at the frame stations, however, resulted in a noticeable improvement in the estimated residual strength. For a load factor of 1.0, the critical lead-crack lengths corresponding to MSD-crack lengths of 0.00 (no MSD), 0.05, 0.10, and 0.20 in. were roughly $2a = 11.6$, 11.1, 10.4, and 9.3 in., respectively. These compare with critical crack lengths of $2a = 6.8$, 6.5, 6.4, and 5.7 in., respectively, for the basic aft-fuselage structure. Hence, the critical lead-crack length for the case involving 0.20 in. MSD cracks was approximately 66.4% longer than that associated with the unreinforced (basic) aft-fuselage configuration. This suggests that incorporation of shear ties in the aft-fuselage section may be an attractive means to increase the residual strength of the structure.

Similarly, incorporation of tear straps also resulted in a significant improvement in residual strength. Figure 17 shows a plot of the estimated residual strength as a function of lead-crack length for a typical aft-fuselage section that has been reinforced with circumferential tear straps at the frame stations and at the midbay locations between frames. For a load factor of 1.0, the critical lead-crack lengths corresponding to MSD-crack lengths of 0.00 (no MSD), 0.05, 0.10, and 0.20 in. were roughly $2a = 13.8$, 13.0, 12.6, and 11.1 in., respectively. These compare with critical crack lengths of $2a = 6.8$, 6.5, 6.4, and 5.7 in., respectively, for the basic aft-fuselage structure and $2a = 11.6$, 11.1, 10.4, and 9.3 in., respectively, for the representative aft-fuselage structure reinforced with shear ties. Hence, the critical lead-crack lengths were nearly double those associated with the unreinforced (basic) aft-fuselage configuration for the prescribed loading. In addition, incorporation of tear straps at the frame *and midbay* locations resulted in an increase in the estimated critical crack lengths that were 18.3–21.5% greater than those associated with incorporation of shear ties at the frame stations. Note that for lead-crack lengths $2a > 17.0$ in., the lead-

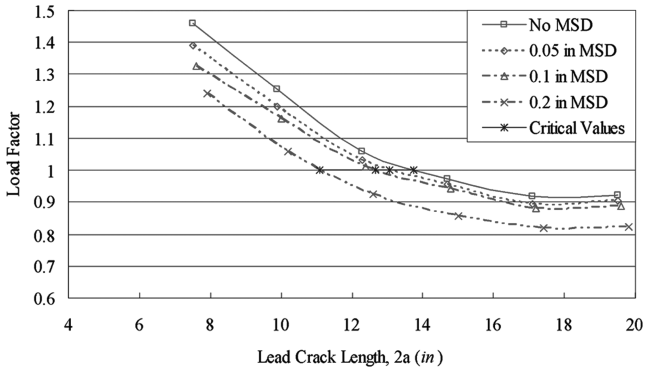

Fig. 17 Estimated residual strength of the representative aft fuselage with tear straps.

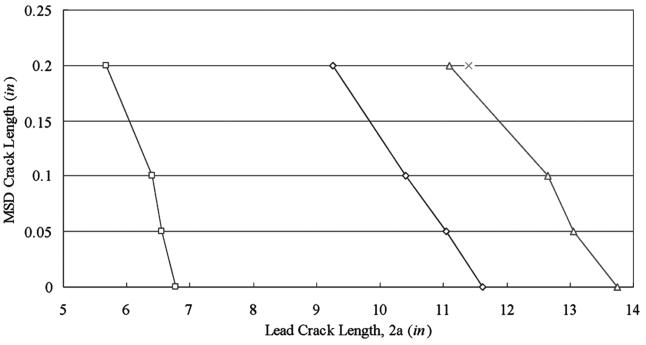

Fig. 19 Zero residual-strength margin for the aft-fuselage lap joint.

crack tips resided underneath the midbay tear strap. This may explain why the residual strength was fairly insensitive to changes in crack length in this region (cf. Fig. 17).

The greatest improvement in residual strength resulted when the aft-fuselage section was reinforced with both shear ties and tear straps. Figure 18 shows a plot of the estimated residual strength as a function of lead-crack length for an aft-fuselage section that has been reinforced with shear ties and tear straps at the frame stations as well as tear straps at the midbay between frames. Similar to the preceding case, the slope of the residual-strength-vs-crack-length curve approaches zero for longer lead-crack lengths. Note, however, that for lead cracks with no MSD and MSD-crack lengths of 0.05 and 0.10 in., the load factor remained greater than unity; that is, the reinforced structure was able to carry the required combined loads over the range of lead-crack lengths considered in this study. For a load factor of 1.0, the critical lead-crack length with 0.20 in. MSD cracks was roughly $2a = 11.4$ in. This compares with critical crack lengths of $2a = 5.7$, 9.1, and 11.1 in., respectively, for the basic, shear-tie, and tear-strap models with 0.20 in. MSD. Clearly, a combination of shear-tie and tear-strap reinforcements provides an alternate load path for redistributing the skin stresses due to the presence of a lead crack in the lap joint.

Using the preceding results, the zero residual-strength margin may be defined as the maximum level of combined damage (i.e., lead-crack length and MSD-crack size) that the fuselage structure can sustain while carrying the limit load (load factor of unity). For the basic and reinforced aft-fuselage lap joints, the zero residual margins are defined as the point at which each residual-strength curve in Figs. 15–18 crosses the horizontal line corresponding to a load factor of 1.0. Figure 19 contains a plot of the zero-residual-strength-margin curves for the unreinforced and reinforced aft-fuselage models. It is clear from the figure that both the shear-tie and tear-strap reinforcements significantly increased the critical crack length for the given required loading and MSD-crack lengths. Note that only one data point is included in Fig. 19 for the combined shear-tie/tear-strap reinforcements. This suggests that the applied loading must be increased to provide enough driving force to extend the considered lead cracks. Table 2 contains a summary of the normalized critical crack lengths for the reinforced aft-fuselage structure a_c/a_{cref}, where a_{cref} is the critical half-crack length for the unreinforced (basic) fuselage structure for a given level of MSD. As can be seen from the table, the three structural reinforcements result in an appreciable increase in the critical crack length for the prescribed loading.

The results presented here suggest that shear ties and tear straps may be effectively used to increase the residual-strength capability of a given fuselage. The reinforcements each provide alternate load paths in the aft fuselage for stress redistribution due to skin cracking; such modifications arguably improve the structural integrity of the original floating-frame construction. Similar conclusions are likely appropriate for the forward- and center-fuselage sections studied by Cope [10] and Lacy et al. [26]. Of course, other issues (ease and cost of installation, weight, etc.) must also be considered to fully assess the proposed structural modifications.

As an aside, the preceding results may be somewhat conservative. Recall that the prescribed kinematic boundary conditions that were applied to the local fuselage boundaries in the material and geometric nonlinear analyses were developed from a linearly elastic finite element model of the global basic model. Because the addition of shear ties and tear straps effectively increases the net cross-sectional area of the fuselage (cf. Table 3), the resultant forces and moments induced on the reinforced local fuselage model boundaries for a given set of applied kinematic boundary conditions are greater than for the basic fuselage. In addition, because the kinematic boundary conditions were developed from a linearly elastic air vehicle model, the stresses induced in a geometric nonlinear analysis will be proportionally larger due to membrane action.

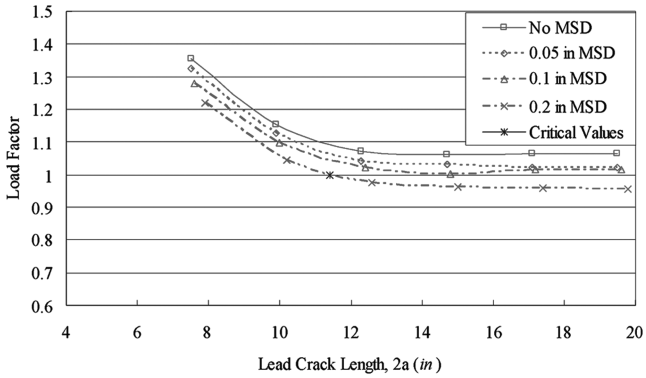

Fig. 18 Estimated residual strength of the representative aft fuselage with a combination of tear straps and shear ties.

Table 2 Normalized critical crack length a_c/a_{cref}

	Normalized critical crack length a_c/a_{cref}		
	Shear ties	Tear straps	Combination
No MSD ($a_{\text{cref}} = 6.8$ in.)	1.714	2.028	N/A
0.05 MSD ($a_{\text{cref}} = 6.6$ in.)	1.687	1.992	N/A
0.10 MSD ($2a_{\text{cref}} = 6.4$ in.)	1.627	1.976	N/A
0.20 MSD ($2a_{\text{cref}} = 5.7$ in.)	1.629	1.954	2.007

Table 3 Cross-sectional area of each retrofit feature model

	Basic	Tear straps	Shear ties	Combination
Area, in.^{2}	1.528	1.848	2.051	2.37
%	100	120.9	134.2	155.1

IV. Conclusions

The residual strength of a typical basic (unreinforced) aft-fuselage section containing a single lead crack decreased substantially with increasing lead-crack length. Based upon the numerical simulations, the presence of MSD cracks resulted in a significant decrease in the fuselage residual strength for a given lead-crack length. Equivalently, the critical crack length for the required limit loading decreased with increasing MSD-crack length. When the aft fuselage was reinforced with shear ties at the frame stations, the critical lead-crack lengths for cases involving varying levels of MSD cracks were at least 60% larger than those associated with the corresponding unreinforced (basic) aft-fuselage configuration.

Similarly, incorporation of circumferential tear straps at the frame stations and at the midbay locations between frames also resulted in a significant improvement in residual strength. The estimated critical lead-crack lengths for cases involving varying levels of MSD cracks were at least 95% longer than those associated with the corresponding unreinforced (basic) aft-fuselage configuration. The tear straps appeared to enhance structural integrity somewhat more than shear-tie reinforcements. This is likely attributable to the fact that tear straps were simulated at the frame stations and at the midbay locations between frames, whereas shear ties were only simulated at the frame stations. As a consequence, for longer lead-crack lengths, the lead-crack and/or MSD-crack tips resided directly underneath the midbay tear strap. These results suggest that incorporation of either shear ties or tear straps in the aft-fuselage section may be an attractive means to increase the residual strength of the floating-frame structure.

The greatest improvement in the estimated residual strength and structural integrity, however, resulted when the aft-fuselage section was reinforced with both shear ties and tear straps at the frame stations and with tear straps at the midbay locations between frames. For the majority of the combinations of lead-crack lengths and MSD-crack lengths considered in this study, the reinforced structure was able to carry the required combined limit loads; this suggests that the applied loading must be increased to provide enough driving force to extend the considered lead cracks. The lone exception was for a single lead crack with 0.20 in. MSD; in this case, the critical crack length was over double that for the corresponding basic fuselage configuration. Hence, a combination of shear-tie and tear-strap reinforcements provides a viable alternate load path for redistributing the skin stresses due to the presence of a lead crack in the lap joint.

These results suggest that shear ties and tear straps may be effectively used to increase the structural integrity of the idealized aft fuselage. Similar conclusions are likely appropriate for other fuselage sections as well. Key results from this study may provide useful information regarding the efficiency of incorporating fail-safe design modifications to enhance the residual strength of cracked sections of the floating-frame fuselages that are similar to those employed on the KC-135 and 707 aircraft. Of course, other factors such as ease and cost of installation, weight penalty, etc., must also be considered to fully assess the proposed structural modifications. Nonetheless, numerical simulations such as those implemented in this study may be used to provide valuable insight into the nonlinear fracture behavior of complex mechanically fastened metallic fuselage structures.

Using a methodology similar to that presented in this work, it may be possible to develop robust residual-strength estimates for complex fuselage structural components with varying levels of in-service damage and MSD/WFD. To fully develop the concepts outlined here, further investigations involving other classes of mechanical joints (double-shear lap joints, butt joints, bonded joints, etc.), optimal modeling of mechanical fasteners, repair assessment, different crack configurations, and other loading cases are warranted. In addition, it will be necessary to consider the effect of crack turning and cyclic loading on the damage-tolerance properties of metallic fuselage structures. Such studies may facilitate optimal fuselage design by providing insight into relationships between material behavior, structural configuration, and crack extension/residual strength that help reduce the risk of catastrophic failure.

References

[1] "USAF Damage Tolerance Design Handbook," Univ. of Dayton Research Inst., Dayton, OH, June 2002.

[2] Broek, D., *The Practical Use of Fracture Mechanics*, Kluwer Academic, Norwell, MA, 1989.

[3] Dawicke, D. S., and Newman, J. C., Jr., "Residual Strength Predictions for Multiple Site Damage Cracking Using a Three-Dimensional Analysis and a CTOA Criterion," *Fatigue and Fracture Mechanics*, Vol. 29, STP 1332, ASTM International, West Conshohocken, PA, 1999, pp. 815–829.

[4] Young, R. D., Rose, C. A., and Starnes, J. H., Jr., "Nonlinear Local Bending Response and Bulging Factors for Longitudinal and Circumferential Cracks in Pressurized Cylindrical Shells," *Third Joint FAA/DoD/NASA Conference on Aging Aircraft*, Albuquerque, NM, NASA Rept. NASA-99-3JCAA-RDY, Sept. 1999, pp. 1–28.

[5] Chen, C., Wawrzynek, P. A., and Ingraffea, A. R., "Crack Growth Simulation and Residual Strength Prediction in Airplane Fuselages," NASA Langley Research Center, Rept. CR-1999-209115, Hampton, VA, Mar. 1999

[6] "General Guidelines for Aircraft Structural Integrity Program," U.S. Air Force, Rept. MIL-HDBK-1530, Nov. 1996.

[7] "Structural Integrity Tests of Pressurized Structure," The Boeing Company, Rept. T-29026, Seattle, WA, Jan. 1958.

[8] "Hydro-Fatigue Test of a KC-135 Fuselage," The Boeing Company, Rept. T6-1245, Seattle, WA, Feb. 1959.

[9] "Fuselage Stress Analysis, Model KC-135," The Boeing Company, Rept. D-16811, Seattle, WA, May 1957.

[10] Cope, D. A., "Fail-Safety and Damage Tolerance Evaluation of KC-135 Fuselage Structure," Ph.D. Dissertation, Dept. of Aerospace Engineering, Wichita State Univ., Wichita, KS, June 2002.

[11] Clapp, B., and Haroldson, B., "Determination of Local Model Boundaries for Fracture Mechanics Analyses of Fuselage Structure," Dept. of Aerospace Engineering, Wichita State Univ., Wichita, KS, Dec. 2001

[12] Dawicke, D. S., and Sutton, M. A., "CTOA and Crack-Tunneling Measurements in Thin Sheet 2024-T3 Aluminum Alloy", *Experimental Mechanics*, Vol. 4, Dec. 1994, pp. 357–368.

[13] Young, R. D., Rose, C. A., and Starnes, J. H., Jr., "Skin, Stringer, and Fastener Loads in Buckled Fuselage Panels," 42nd AIAA Structures, Structural Dynamics, and Materials Conference, AIAA Paper 2001-1326, Apr. 2001.

[14] Carter, B. J., Chen, C.-S., Wawrzynek, P. A., and Ingraffea, A. R., "A Topology-Based System for Modeling 3-D Crack Growth in Solid and Shell Structures," *Proceedings of the Ninth International Congress on Fracture (ICF9)*, Elsevier, New York, 1997, pp. 1923–1934.

[15] Rankin, C. C., Brogan, F. A., Loden, W. A., and Cabiness, H. D., "STAGS User Manual, Ver. 4.0," Advanced Technology Center, Lockheed Martin Missiles and Space, Palo Alto, CA, June 2000.

[16] Starnes, J. H., Jr., Britt, V. O., Rose, C. A., and Rankin, C. C., "Non-Linear Response and Residual Strength of Damaged Stiffened Shells Subjected to Combined Loads," 37th AIAA Structures, Structural Dynamics, and Materials Conference, AIAA Paper 96-1555, Apr. 1996, pp. 2096–2111.

[17] Potyondy, D. O., "A Methodology for Simulation of Curvilinear Crack Growth in Pressurized Shells," Ph.D. Thesis, Cornell Univ., Ithaca, NY, Aug. 1993.

[18] Dawicke, D. S., "Residual Strength Predictions Using a Crack Tip Opening Angle Criterion," *FAA-NASA Symposium on the Continued Airworthiness of Aircraft Structure*, DOT/FAA AR-97/2, Vol. 2, U.S. Dept. of Transportation, Federal Aviation Administration, Atlantic City, NJ, July 1997, pp. 555–566.

[19] Potyondy, D. O., Wawrzynek, P. A., and Ingraffea, A. R., "Discrete Crack Growth Analysis Methodology for Through Cracks in Pressurized Fuselage Structures," *International Journal for Numerical Methods in Engineering*, Vol. 38, No. 10, 1995, pp. 1611–1633. doi:10.1002/nme.1620381003

[20] Newman, J. C., Jr., "An Elastic-Plastic Finite Element Analysis of Crack Initiation, Stable Crack Growth, and Instability," *Fracture Mechanics: Fifteenth Symposium*, STP 833, ASTM International, West Conshohocken, PA, 1984, pp. 93–117.

[21] Newman, J. C., Jr., and James, M., "A Review of the CTOA/CTOD Fracture Criterion," 42nd AIAA Structures, Structural Dynamics, and Materials Conference, AIAA Paper 2001-1324, Apr. 2001.

[22] Seshadri, B. R., and Newman, J. C., Jr., "Residual Strength Analyses of Riveted Lap-Splice Joints," *Fatigue and Fracture Mechanics*, Vol. 31,

STP 1389, ASTM International, West Conshohocken, PA, 2000, pp. 486–504.

[23] Dawicke, D. S., Gullerud, A. S., Dodds, R. H., Jr., and Hampton, R. W., "Residual Strength Predictions with Crack Buckling," *Second Joint NASA/FAA/DoD Conference on Aging Aircraft*, CP-1999-208982, NASA Langley Research Center, Hampton, VA, Jan. 1999, pp. 565–574.

[24] Young, R. D., Rouse, M., Ambur, D. R., and Starnes, J. H., Jr., "Residual Strength Pressure Tests and Non-Linear Analyses of Stringer- and Frame-Stiffened Aluminum Fuselage Panels with Longitudinal Cracks," *Second Joint NASA/FAA/DoD Conference on Aging Aircraft*, CP-1999-208982, NASA Langley Research Center, Hampton, VA, Jan. 1999, pp. 408–426.

[25] Cope, D. A., and Lacy, T. E., "Modeling Mechanical Fasteners in Single-Shear Lap Joints," *Journal of Aircraft*, Vol. 41, No. 6, Nov. 2004, pp. 1491–1497. doi:10.2514/1.14435

[26] Lacy, T. E., Cope, D. A., Hijazi, A., and Yamada, Y., "Evaluation and Retro-Fit of Fail-Safety on KC-135 Fuselage Structure," College of Engineering, Wichita State Univ. Rept. WSU 4493, Wichita, KS, 2002.

[27] Swift, T., "Damage Tolerance in Pressurized Fuselages," *14th Symposium of the International Committee on Aeronautical Fatigue*, EMAS Publishing, Warley, England, U.K., 8–12 June 1987, pp. 1–77.

[28] Swift, T., "Widespread Fatigue Damage Monitoring—Issues and Concerns," *FAA/NASA International Symposium on Advanced Structural Integrity Methods for Airframe Durability and Damage Tolerance*, CP-3274, NASA Langley Research Center, Hampton, VA, Sept. 1994, pp. 829–870.

[29] Swift, T., "Fracture Analysis of Stiffened Structures," *Damage Tolerance of Metallic Structures: Analysis Methods and Application*, STP 842, ASTM International, West Conshohocken, PA, 1984, pp. 69–107.